Efficient dual-stage all-solid-state post-compression for 100 W level ultrafast laser

Zichen Gao[1,2], Jie Guo[1], Yongxi Gao[1,2], Yuguang Huang[1,2], Zhihua Tu[1,3], and Xiaoyan Liang[1]

[1] *State Key Laboratory of High Field Laser Physics and CAS Center for Excellence in Ultra-intense Laser Science, Shanghai Institute of Optics and Fine Mechanics, Chinese Academy of Sciences, Shanghai 201800, China*

[2] *Center of Materials Science and Optoelectronics Engineering, University of Chinese Academy of Sciences, Beijing 100049, China*

[3] *School of Physics Science and Engineering, Tongji University, Shanghai 200092, China*

Abstract We demonstrate an efficient and economical all-solid-state post-compression based on a dual-stage periodically placed thin fused silica plates driven by a >100 W Yb:YAG Innoslab amplifier seeded by a fiber frontend. Not only >8-fold pulse compression with 94% transmission is achieved, the pulse quality and spatial mode are also improved, which can be attributed to the compensation for the residual high-order dispersion and the spatial mode self-cleaning effect during the nonlinear process. It enables a high-power ultrafast laser source with 64 fs pulse duration, 96 W average power at 175 kHz repetition rates, and good spatiotemporal quality. These results highlight this all-solid-state post-compression can overcome the bandwidth limitation of Yb-based laser with exceptional efficiency and mitigate the spatiotemporal degradation originating from the Innoslab amplifier and fiber frontend, which provides an efficient and economical complement for the Innoslab laser system and facilitates this robust and compact combination as a promising scheme for high-quality higher-power few-cycle lasers generation.

Key words: post-compression; self-focusing effect; high power ultrafast source

Correspondence to: J. Guo and X. Liang, No. 390 Qinghe Road, Jiading, Shanghai,201800, China. Email: gracejie123@siom.ac.cn (J. Guo); liangxy@siom.ac.cn (X. Liang)

1. Introduction

High-power ultrafast laser sources are highly demand tools in various ultrafast applications [1-3]. The high peak power enables these applications to be driven, while the high average power satisfies their need for high photon flux and high signal-to-noise ratio. Thanks to the high quantum and Stokes efficiency, as well as the excellent thermal management of state-of-the-art fiber, thin-disk, and Innoslab laser architectures, Yb-based lasers are capable of reaching several hundred watts, and even >1 kW[4-7].

The solid-state amplifiers shine in terms of high pulse energy owing to negligible nonlinear effect and high damage threshold of key devices, especially the Innoslab amplifier endowed with the compact configuration and high amplification factor. The fiber laser can work as an outstanding frontend owing to its robustness, excellent beam quality, and the integration of chirped fiber Bragg gratings (CFBGs) as the stretcher without misaligning like the grating stretcher. Hence, the Innoslab amplifier seeded by a fiber frontend provides an attractive choice for achieving a superior high-power laser system [8-10]. However, there are still some drawbacks that cannot be ignored. First, the narrow gain bandwidth limits the generation of sub-100 fs ultrashort pulses, which is a common drawback of Yb-based lasers. Second, the compressed pulses always show the obvious pedestals which can be attributed to the inability of grating compressor in offsetting the higher-order dispersion mainly from fiber frontend. Finally, the output beam of Innoslab amplifier is always elliptical and accompanied with spatial distortion. The implementation of high-quality beam generally requires the state-of-the-art reshaping and spatial filtering.

The post-compression technology is an effective route for overcoming the narrow bandwidth limitation, which mainly relies on the spectral broadening by self-phase modulation (SPM). Due to the long-distance nonlinear effect with gas medium and the waveguide structure, many pulse compression results with large compression factor and high spatial quality are demonstrated by the gas-filled hollow core fiber technology [11-14]. However, the low fiber coupling efficiency, alignment sensitivity and increased susceptibility to damage at high power are the inescapable drawbacks, which restrict its application to high power lasers. The multi-pass cell approach is also a widely applied technique [15-21]. In contrast, high transmission efficiency pulse compression can be achieved because of the absence of fiber coupling loss. Nonetheless, the large number of reflections on the cavity mirrors require a state-of-the-art coating with high reflectivity and low (or negative) group-delay dispersion, which is costly and technically challenging. Impressive performances are also shown in multi-thin-solid-plates (MTSP) technique which is simple, robust and economical [22-26]. But the MTSP technique usually need an elaborate strategy in placing the thin plates to avoid the catastrophic spatial Kerr effect which can cause energy loss, beam deterioration and irreversible material damage [27-30]. Vlasov et al. proposed a periodical self-focusing system where a repeating (stationary) propagation is achieved by balancing the spatial nonlinear effect and beam divergence, which allows a high-efficiency spectral broadening without catastrophic self-focusing effect even though the peak power far beyond the self-focusing critical power[27]. Zhang et al. introduced the Fresnel-Kirchhoff diffraction (FKD) integral to identify a more exact solution and demonstrated an 8-fold pulse compression with >85% efficiency[28]. In our previous work, we proposed a simple Gaussian beam optics model to find the solution from a more practical perspective and demonstrated a 17-fold pulse compression with 94% efficiency[30].

In this work, we demonstrate a dual-stage periodically placed thin fused silica plates post-compression used for the Innoslab laser system seeded by a fiber frontend, eventually implementing an efficient, compact and robust high-power ultrafast laser source with 64 fs pulse duration and 96 W average power at 175 kHz repetition rate. The high average power laser is provided by the compact Innoslab laser system, but the spatial quality degraded from the amplification process and temporal quality is undesirable because of the mismatched spectral phase between the stretcher and grating compressor. Not only >8-fold pulse compression is achieved with 94% transmission, the spatial mode and pulse quality are also improved in the dual-stage all-solid-state post-compression. In time domain, the final pulses are almost pedestal-free and quite close to Fourier-transform-limited (FTL) pulse duration, because the compensation for high-order dispersion during the nonlinear process. In space domain, the increasingly circular and clean beam profile can be attributed to spatial mode self-cleaning effect. Similar effect was reported in [28], which was considered as the effort of spatial self-organization of laser beam and previously observed in the nonlinear process of filamentation[31], self-focusing collapse[32] and multimode fibers[33]. This spatial improvement resulting in the increase of spatial energy concentration, which strengthens the application of the Innoslab laser system. These results demonstrate the periodically placed thin-solid-plates post-compression is competent to overcome the narrow bandwidth limitation of Yb-based laser with exceptional efficiency and enable a high-quality laser output by the spatiotemporal self-cleaning effect. This work indicates that the periodically placed thin-solid-plates post-compression is an efficient and economical complement for the Innoslab laser system and this robust and compact combination may be a promising scheme for generating the higher power few-cycle lasers with good spatial and temporal quality.

2.   Experimental setup

As illustrated in the Fig. 1, the efficient all-solid-state post-compression based on dual-stage periodically placed fused silica plates is used for a high-power Yb:YAG Innoslab laser system which is seeded by a commercial all-fiber frontend, eventually yielding a high-power ultrafast laser output.
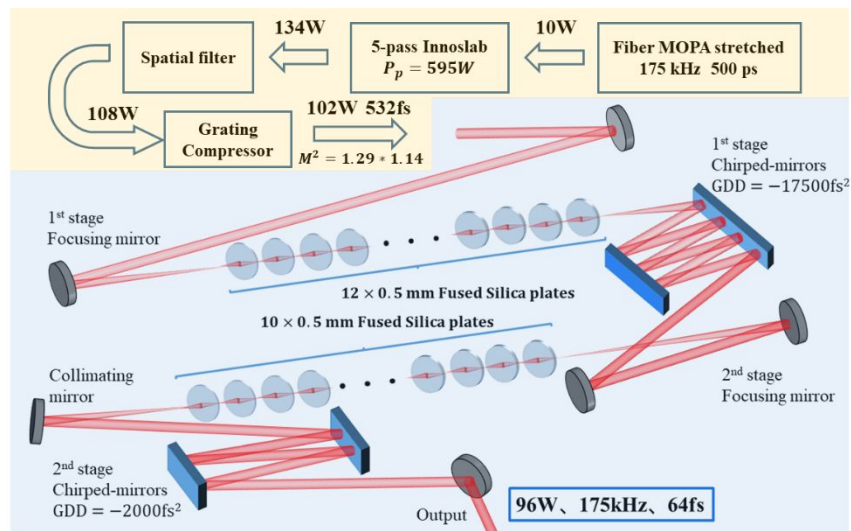

Fig. 1 Schematic of experimental setup. The high-power ultrafast laser output is achieved by the dual-stage all-solid-state post-compression (blue shaded) driven by a >100W average power Yb:YAG Innoslab amplifier system (yellow shaded).

The high-power amplifier system is described in detail in [34], which employs chirped pulse amplification, spatial filter and grating compressor. It delivers 102 W average power at 175 kHz repetition rate，corresponding to a pulse energy ~0.6 mJ. The amplifier output spectrum is shown in the Fig. 3(a) of the following section, which is centered at 1030 nm and corresponds to a FTL pulse duration of 250 fs. The autocorrelation trace is shown in Fig. 2(a), indicating 532 fs pulses with pedestals assuming a Lorentz pulse shape (APE GmbH, pulseCheck-NX50), which is larger than the FTL pulse duration (factor~2.1). This can be attributed to the nonlinear effect of fiber frontend and the mismatch in higher-order dispersion between grating compressor and CFBGs. The amplifier output beam quality is characterized as $M^2=1.29*1.14$ (Ophir BeamSquared), as shown in Fig. 2(b). Although it is nearly diffraction-limited after spatial reshaping and filtering, a few high-order spatial modes and spatial distortion are difficult to completely eliminate, as evidenced by the images measured at different locations.
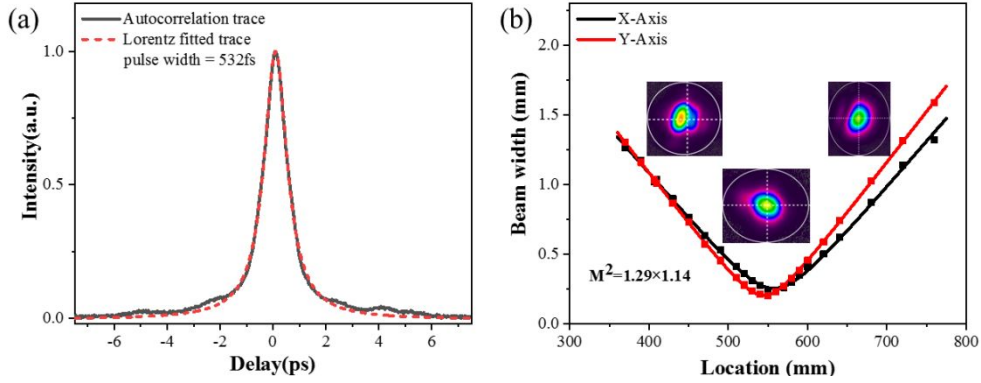

Fig. 2. (a) Measured and Lorentz fitted autocorrelation traces and (b) the beam quality after grating compressor

The dual-stage all-solid-state post-compression consists of periodically placed thin solid plates for nonlinear spectral broadening, focusing mirrors for mode-matching and chirped mirrors for dispersion compensation. The first stage mode-matching is achieved by a curved mirror with 2500 mm radius of curvature (ROC), focusing the beam to a waist with 0.5 mm diameter. In the first-stage spectral broadening system, twelve 0.5 mm thickness fused silica plates are periodically arranged with a distance of 40 mm, i.e. the period of system. In order to maximize the transmission efficiency, these uncoated plates are all placed at Brewster angle and the laser is linearly p-polarized. Placing the first plate 20 mm behind the waist, thereby the stationary mode will propagate in the system at the balance of the self-focusing effect and diffraction when the full power applied, which enables the high-efficiency spectral broadening with high spatial quality. The second-stage one comprises ten 0.5 mm thickness fused silica plates at a period of 75 mm. The mode-matching condition is placing the first plate of the second-stage spectral broadening system 38mm behind a 0.7 mm diameter waist formed by a 4000 mm ROC curved mirror, corresponding an estimated peak intensity of about 1TW/cm^2 on the plates which is similar to that of the first stage. Above-mentioned mode-matching condition and spectral broadening system design are all determined by the Gaussian beam optics model detailed in [30]. It identifies the stationary mode propagation by approximating the spatial Kerr effect of thin-solid plates as a nonlinear lens group. The focal length can be expressed by[35]

$$f \approx \frac{hw^2}{4n_2 I_0 l_{eff}}$$ (1)

Where ω is the beam radius on the plates, n_2 is nonlinear refractive index, I_0 is peak intensity, l is the nonlinear length per plate, and h is a correlator factor used to account for the higher order terms ignored in the parabolic approximation. According to [36], h=5 when B is close to 1, making it a general solution for low B-integral accumulation per plate situations. The strong space-time coupling can also be avoided in the low B-integral situation. In this dual-stage system, the estimated equivalent focal lengths are about 20 mm and 38 mm, respectively.

The spectrally broadened pulses are compressed by chirped mirrors where the first-stage compressor provides a total group delay dispersion (GDD) of -17500 fs² and that of second-stage compressor is -2000 fs². The reason why numerous chirped mirrors are employed in the first-stage compressor is the massive residual GDD after grating compressor. If the GDD is completely offset in the grating compressor, an obvious pedestal and many sidelobe pulses with considerable intensity will appear in addition to a narrower center-peak pulse, which are mainly caused by the residual third-order dispersion (TOD) and higher-order dispersion. During the nonlinear process, the nonlinear induced dispersion can offset the residual high-order dispersion to some extent. According to the theory of [37], the residual TOD after nonlinear process decreases to a negligible level of $10^{-6} \sim 10^{-7}$ ps³ with the accumulation of nonlinear effect, eventually resulting in the pulse self-cleaning even though chirped mirrors only offset GDD. As a result, the dispersion to be compensated in the second-stage compressor is substantially reduced thanks to the pulse-cleaning in the first stage.

3. Results and discussions

The spectral evolution of the high-power ultrafast system is illustrated in Fig. 3(a). An obvious gain narrowing is introduced as the power enhancement in the Yb:YAG Innoslab amplifier and the spectral bandwidth is narrowed to 2.9 nm (full width at half maximum, FWHM) from the 8.3 nm (FWHM) of the seed. After dual-stage periodically placed fused silica plates, the spectrum is significantly broadened due to the SPM effect. The first-stage spectral broadening basically offsets the impact of gain narrowing, extending the spectral range close to that of seed. The second-stage exhibits stronger ability on spectral broadening, eventually broadening the spectral range to the range of 990-1065 nm at -20 dB level. Although the accumulated B-integral is similar, the spectral broadening effectiveness shown in dual-stage is quite different. This can be attributed to the massive residual chirp in the first-stage initial pulses, which weaken the capability of spectral broadening[38]. The asymmetry of spectral broadening is caused by the high-order dispersion of initial pulses and the self-steepening effect[37, 38]. Fig. 3(b) shows the good spatial homogeneity of spectral broadening, which is characterized by the spectra measured across the transverse beam profile of final output beam at the location with a beam radius of about 6 mm, indicating the spatial chirp is well controlled by the strategically placed thin plates.
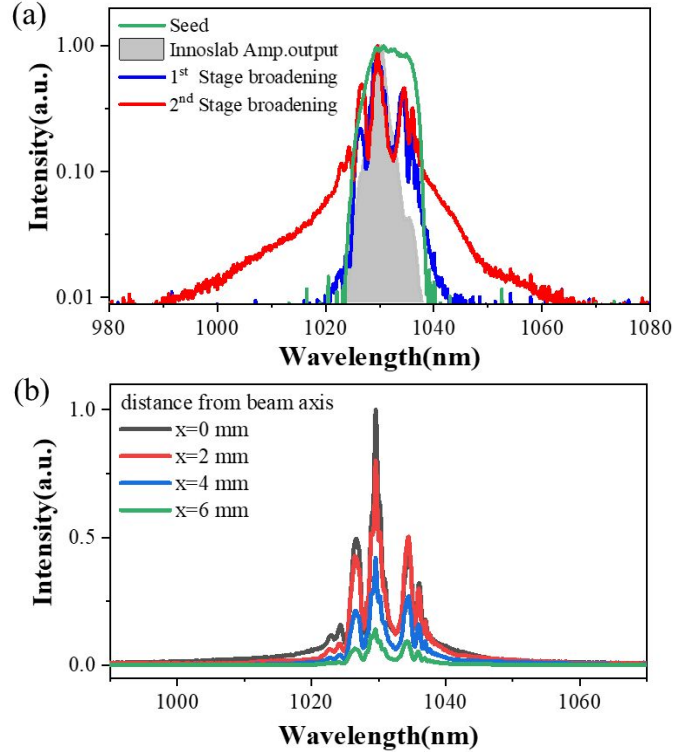
Fig. 3 (a) Spectra measured at the output of fronted, amplifier, first-stage and second-stage spectral broadening. (b) Spectra across the final output beam profile.

The measured and Lorentz fitted autocorrelation traces characterized at the first-stage and second-stage post-compression are shown in Fig. 4. After the first-stage post-compression, the pulses are actually compressed to 239 fs, which is larger than the FTL pulse duration (factor~1.3) and corresponds to a compression factor of 2. Although the first-stage spectral broadening is slight, the much shorter pulses can be achieved due to the nonlinear dispersion compensation. Compared with the initial pulse, the pulse width is closer to FTL pulse duration and pedestals are cleaned to some degree. As shown in Fig. 4 (b), the pedestal-free pulses of 64 fs are measured after the second-stage post-compression, corresponding to a 4-fold pulse compression. The pulse width is very close to the FTL pulse duration (factor ~ 1.07), and the pedestals of amplifier output pulses are almost completely cleaned. These results indicate that the dual-stage all-solid-state post-compression achieves not only a large factor pulse compression but also a pulse-cleaning effect for the driving pulse quality stemmed from the fiber frontend. The pulse-cleaning effect is introduced by the high-order dispersion compensation in the nonlinear process[37], making the ultrafast pulses with a pulse width closer to FTL pulse duration and cleaner pedestals in the case only the negative GDD can be provided in the chirped-mirrors compressor.
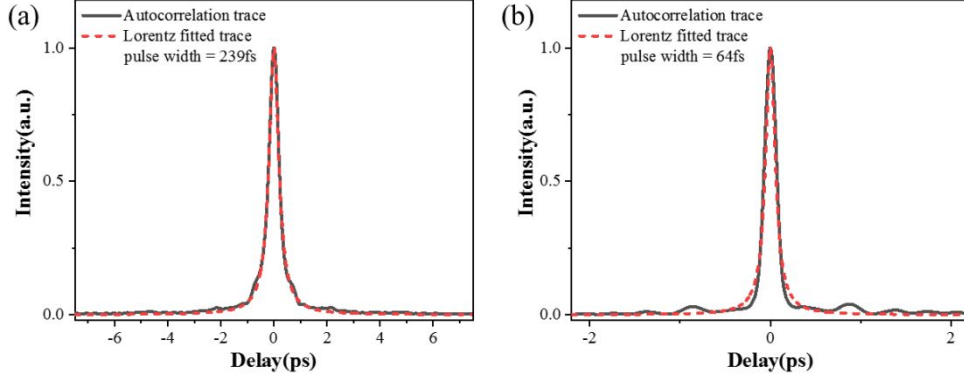
6

Fig. 4 Measured and Lorentz fitted autocorrelation traces of (a) the first-stage and (b) second-stage post compression.

The beam quality and beam profile at different stages are illustrated in Fig. 5. The first-stage output beam quality is measured to be $M^2=1.42*1.28$ and that of second-stage output is $M^2=1.53*1.38$. The beam profiles are measured at the near field, focal spot and after focus respectively. The M^2 factor increases slightly with the nonlinear propagation in the system, while the spatial mode is significantly improved. The beam profiles are no longer elliptical and the sidelobes and spatial distortion have been almost eliminated. The similar spatial mode self-cleaning effect in the periodically placed thin-solid-plates was also reported in [28] and previously observed in other nonlinear process[31-33]. According to the investigation of [28], the spatial mode self-cleaning effect only occurs during stationary mode propagation in the periodically placed thin-solid-plates and can be attributed to the spatial self-organization effect in this waveguide-like propagation.
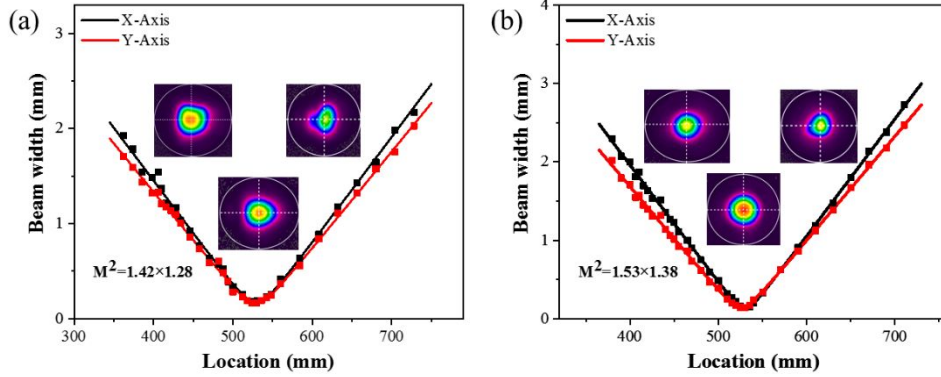

Fig. 5 Beam quality measured after (a) first-stage and (b) second-stage post-compression.

To further investigate this nonlinear spatial mode self-cleaning effect, we measured the evolution of beam profile at different locations and final beam quality with the increase of power, as shown in Fig. 6. The spatial mode self-cleaning effect can also be observed in this power-related evolution, which becomes more apparent as the power approaches the design conditions. The beam profile is becoming increasingly circular and clean regardless of at near field, focal spot, and after focus, which indicates an improvement of spatial mode. Although the increase of M^2 factor cannot be completely avoided due to the intensity-dependent spatial nonlinear effect, only a slight change would be introduced by controlling the accumulated B-integral per plates whose impacts can be ignored in the applications[15]. Following the dual-stage post-compression, the final output average power is 96 W, demonstrating an exceptional efficiency of 94%. This high-efficiency spatial mode self-cleaning effect in the post-compression is quite suitable for the Innoslab laser

7

system, which overcomes the limitations of narrow gain width and improves the spatial mode simultaneously. These results suggest that only this nonlinear effect used for the spatial filtering without additional spatial filtering modules like a slit may be feasible, which would significantly enhance the overall efficiency and unleash the power-boost capability of this high-power laser system.
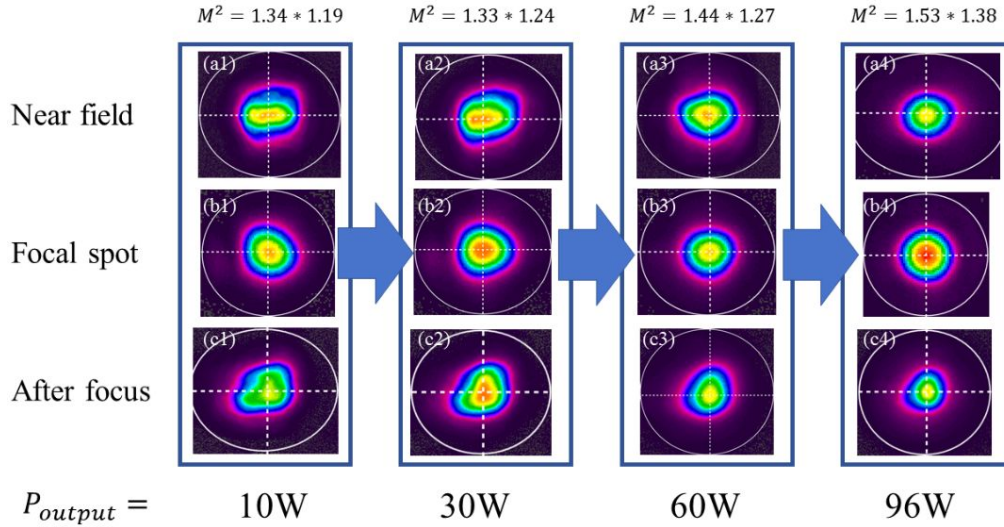

Fig. 6 Evolution of beam quality and beam profile at different locations with the output power.

4.   Summary

In summary, we demonstrate an efficient all-solid-state post-compression based on a dual-stage periodically placed thin-solid-plates. It is driven by a compact and robust Yb:YAG Innoslab laser system which is seeded by a fiber frontend and yields a 100 W-level average power with mJ-level pulse energy. This economical all-solid-state post-compression not only achieves a >8-fold pulse compression with exceptional efficiency of 94%, but also improves the spatial mode and pulse quality of this high-power laser system which are helpful in many applications. Eventually, an efficient, robust, and compact high-power ultrafast laser source is implemented with 64 fs pulse duration, 96 W average power at 175 kHz repetition rate, good spatial mode and pulse quality. This work proves the potentiality of periodically placed thin-solid-plates post-compression combined with the Innoslab laser seeded on a fiber frontend in enabling the generation of efficient, robust, and compact laser source with higher power, few-cycle pulses, and good spatial and temporal quality.

Acknowledgement

References

1. T. Saule, S. Heinrich, J. Schötz, N. Lilienfein, M. Högner, O. deVries, M. Plötner, J. Weitenberg, D. Esser, J. Schulte, P. Russbueldt, J. Limpert, M. F. Kling, U. Kleineberg, and I. Pupeza, "High-flux ultrafast extreme-ultraviolet photoemission spectroscopy at 18.4 MHz pulse repetition rate," Nature Communications 10, 458 (2019). DOI: https://doi.org/10.1038/s41467-019-08367-y

2. T. Popmintchev, M.-C. Chen, D. Popmintchev, P. Arpin, S. Brown, S. Ališauskas, G. Andriukaitis, T. Balčiunas, O. D. Mücke, A. Pugzlys, A. Baltuška, B. Shim, S. E. Schrauth, A. Gaeta, C. Hernández-García, L. Plaja, A. Becker, A. Jaron-Becker, M. M. Murnane, and H. C. Kapteyn, "Bright Coherent Ultrahigh Harmonics in the keV X-ray Regime from Mid-Infrared Femtosecond Lasers," Science 336, 1287-1291 (2012). DOI: https://doi.org/10.1126/science.1218497

3. S. Mikaelsson, J. Vogelsang, C. Guo, I. Sytcevich, A.-L. Viotti, F. Langer, Y.-C. Cheng, S. Nandi, W. Jin, A. Olofsson, R. Weissenbilder, J. Mauritsson, A. L'Huillier, M. Gisselbrecht, and C. L. Arnold, "A high-repetition rate attosecond light source for time-resolved coincidence spectroscopy," Nanophotonics 10, 117-128 (2021). DOI: https://doi.org/doi:10.1515/nanoph-2020-0424

4. H. Stark, J. Buldt, M. Muller, A. Klenke, and J. Limpert, "1 kW, 10 mJ, 120 fs coherently combined fiber CPA laser system," Opt Lett 46, 969-972 (2021). DOI: https://doi.org/10.1364/OL.417032

5. P. Russbueldt, T. Mans, J. Weitenberg, H. D. Hoffmann, and R. Poprawe, "Compact diode-pumped 1.1 kW Yb:YAG Innoslab femtosecond amplifier," Opt. Lett. 35, 4169-4171 (2010). DOI: https://doi.org/10.1364/OL.35.004169

6. C. Röcker, A. Loescher, F. Bienert, P. Villeval, D. Lupinski, D. Bauer, A. Killi, T. Graf, and M. Abdou Ahmed, "Ultrafast green thin-disk laser exceeding 1.4 kW of average power," Opt. Lett. 45, 5522-5525 (2020). DOI: https://doi.org/10.1364/OL.403781

7. T. Nubbemeyer, M. Kaumanns, M. Ueffing, M. Gorjan, A. Alismail, H. Fattahi, J. Brons, O. Pronin, H. G. Barros, Z. Major, T. Metzger, D. Sutter, and F. Krausz, "1 kW, 200 mJ picosecond thin-disk laser system," Opt. Lett. 42, 1381-1384 (2017). DOI: https://doi.org/10.1364/OL.42.001381

8. K. Mecseki, M. K. R. Windeler, A. Miahnahri, J. S. Robinson, J. M. Fraser, A. R. Fry, and F. Tavella, "High average power 88 W OPCPA system for high-repetition-rate experiments at the LCLS x-ray free-electron laser," Opt. Lett. 44, 1257-1260 (2019). DOI: https://doi.org/10.1364/OL.44.001257

9. B. E. Schmidt, A. Hage, T. Mans, F. Légaré, and H. J. Wörner, "Highly stable, 54mJ Yb-InnoSlab laser platform at 0.5kW average power," Opt. Express 25, 17549-17555 (2017). DOI: https://doi.org/10.1364/OE.25.017549

10. Y. Gao, J. Guo, Y. Huang, Z. Gao, Z. Gan, Z. Tu, X. Liang, and R. Li, "417 W, 2.38 mJ Innoslab amplifier compressible to a high pulse quality of 406 fs," Opt. Lett. 48, 5328-5331 (2023). DOI: https://doi.org/10.1364/OL.503761

11. T. Balciunas, C. Fourcade-Dutin, G. Fan, T. Witting, A. A. Voronin, A. M. Zheltikov, F. Gerome, G. G. Paulus, A. Baltuska, and F. Benabid, "A strong-field driver in the single-cycle regime based on self-compression in a kagome fibre," Nature Communications 6, 6117 (2015). DOI: https://doi.org/10.1038/ncomms7117

12. T. Nagy, S. Hädrich, P. Simon, A. Blumenstein, N. Walther, R. Klas, J. Buldt, H. Stark, S. Breitkopf, P. Jójárt, I. Seres, Z. Várallyay, T. Eidam, and J. Limpert, "Generation of

three-cycle multi-millijoule laser pulses at 318 W average power," Optica 6, 1423-1424 (2019). DOI: https://doi.org/10.1364/OPTICA.6.001423

13. M. Ouillé, A. Vernier, F. Böhle, M. Bocoum, A. Jullien, M. Lozano, J.-P. Rousseau, Z. Cheng, D. Gustas, A. Blumenstein, P. Simon, S. Haessler, J. Faure, T. Nagy, and R. Lopez-Martens, "Relativistic-intensity near-single-cycle light waveforms at kHz repetition rate," Light: Science & Applications 9, 47 (2020). DOI: https://doi.org/10.1038/s41377-020-0280-5

14. Z. Pi, H. Y. Kim, and E. Goulielmakis, "Petahertz-scale spectral broadening and few-cycle compression of Yb:KGW laser pulses in a pressurized, gas-filled hollow-core fiber," Opt. Lett. 47, 5865-5868 (2022). DOI: https://doi.org/10.1364/OL.474872

15. P. Russbueldt, J. Weitenberg, J. Schulte, R. Meyer, C. Meinhardt, H. D. Hoffmann, and R. Poprawe, "Scalable 30 fs laser source with 530 W average power," Opt. Lett. 44, 5222-5225 (2019). DOI: https://doi.org/10.1364/OL.44.005222

16. M. Kaumanns, D. Kormin, T. Nubbemeyer, V. Pervak, and S. Karsch, "Spectral broadening of 112 mJ, 1.3 ps pulses at 5 kHz in a LG10 multipass cell with compressibility to 37 fs," Opt. Lett. 46, 929-932 (2021). DOI: https://doi.org/10.1364/OL.416734

17. M. Müller, J. Buldt, H. Stark, C. Grebing, and J. Limpert, "Multipass cell for high-power few-cycle compression," Opt. Lett. 46, 2678-2681 (2021). DOI: https://doi.org/10.1364/OL.425872

18. S. Rajhans, E. Escoto, N. Khodakovskiy, P. K. Velpula, B. Farace, U. Grosse-Wortmann, R. J. Shalloo, C. L. Arnold, K. Põder, J. Osterhoff, W. P. Leemans, I. Hartl, and C. M. Heyl, "Post-compression of multi-millijoule picosecond pulses to few-cycles approaching the terawatt regime," Opt. Lett. 48, 4753-4756 (2023). DOI: https://doi.org/10.1364/OL.498042

19. L. Silletti, A. bin Wahid, E. Escoto, P. Balla, S. Rajhans, K. Horn, L. Winkelmann, V. Wanie, A. Trabattoni, C. M. Heyl, and F. Calegari, "Dispersion-engineered multi-pass cell for single-stage post-compression of an ytterbium laser," Opt. Lett. 48, 1842-1845 (2023). DOI: https://doi.org/10.1364/OL.476846

20. K. Fritsch, M. Poetzlberger, V. Pervak, J. Brons, and O. Pronin, "All-solid-state multipass spectral broadening to sub-20 fs," Opt. Lett. 43, 4643-4646 (2018). DOI: https://doi.org/10.1364/OL.43.004643

21. A.-L. Viotti, C. Li, G. Arisholm, L. Winkelmann, I. Hartl, C. M. Heyl, and M. Seidel, "Few-cycle pulse generation by double-stage hybrid multi-pass multi-plate nonlinear pulse compression," Opt. Lett. 48, 984-987 (2023). DOI: https://doi.org/10.1364/OL.478790

22. J. E. Beetar, S. Gholam-Mirzaei, and M. Chini, "Spectral broadening and pulse compression of a 400 μJ, 20 W Yb:KGW laser using a multi-plate medium," Applied Physics Letters 112, 051102 (2018). DOI: https://doi.org/10.1063/1.5018758

23. S. Tóth, R. S. Nagymihály, I. Seres, L. Lehotai, J. Csontos, L. T. Tóth, P. P. Geetha, T. Somoskői, B. Kajla, D. Abt, V. Pajer, A. Farkas, Á. Mohácsi, Á. Börzsönyi, and K. Osvay, "Single thin-plate compression of multi-TW laser pulses to 3.9 fs," Opt. Lett. 48, 57-60 (2023). DOI: https://doi.org/10.1364/OL.478253

24. C.-H. Lu, W.-H. Wu, S.-H. Kuo, J.-Y. Guo, M.-C. Chen, S.-D. Yang, and A. H. Kung, "Greater than 50 times compression of 1030 nm Yb:KGW laser pulses to single-cycle

duration," Opt. Express 27, 15638-15648 (2019). DOI: https://doi.org/10.1364/OE.27.015638

25. M. Seo, K. Tsendsuren, S. Mitra, M. Kling, and D. Kim, "High-contrast, intense single-cycle pulses from an all thin-solid-plate setup," Opt. Lett. 45, 367-370 (2020). DOI: https://doi.org/10.1364/OL.382592

26. C.-H. Lu, Y.-J. Tsou, H.-Y. Chen, B.-H. Chen, Y.-C. Cheng, S.-D. Yang, M.-C. Chen, C.-C. Hsu, and A. H. Kung, "Generation of intense supercontinuum in condensed media," Optica 1, 400-406 (2014). DOI: https://doi.org/10.1364/OPTICA.1.000400

27. S. N. Vlasov, V. A. Petrishchev, and V. I. Talanov, "Theory of Periodic Self-Focusing of Light Beams," Appl. Opt. 9, 1486-1488 (1970). DOI: https://doi.org/10.1364/AO.9.001486

28. S. Zhang, Z. Fu, B. Zhu, G. Fan, Y. Chen, S. Wang, Y. Liu, A. Baltuska, C. Jin, C. Tian, and Z. Tao, "Solitary beam propagation in periodic layered Kerr media enables high-efficiency pulse compression and mode self-cleaning," Light: Science & Applications 10, 53 (2021). DOI: https://doi.org/10.1038/s41377-021-00495-9

29. J. Guo, Z. Gao, D. Sun, X. Du, Y. Gao, and X. Liang, "An efficient high-power femtosecond laser based on periodic-layered-Kerr media nonlinear compression and a Yb:YAG regenerative amplifier," High Power Laser Science and Engineering 10, e10 (2022). DOI: https://doi.org/10.1017/hpl.2022.3

30. Z. Gao, J. Guo, Y. Gao, and X. Liang, "Efficient nonlinear pulse compression to 20 fs based on an all-solid-state periodic self-focusing system," Optics & Laser Technology 175, 110714 (2024). DOI: https://doi.org/https://doi.org/10.1016/j.optlastec.2024.110714

31. B. Prade, M. Franco, A. Mysyrowicz, A. Couairon, H. Buersing, B. Eberle, M. Krenz, D. Seiffer, and O. Vasseur, "Spatial mode cleaning by femtosecond filamentation in air," Opt. Lett. 31, 2601-2603 (2006). DOI: https://doi.org/10.1364/OL.31.002601

32. K. D. Moll, A. L. Gaeta, and G. Fibich, "Self-Similar Optical Wave Collapse: Observation of the Townes Profile," Physical Review Letters 90, 203902 (2003). DOI: https://doi.org/10.1103/PhysRevLett.90.203902

33. K. Krupa, A. Tonello, B. M. Shalaby, M. Fabert, A. Barthélémy, G. Millot, S. Wabnitz, and V. Couderc, "Spatial beam self-cleaning in multimode fibres," Nature Photonics 11, 237-241 (2017). DOI: https://doi.org/10.1038/nphoton.2017.32

34. Y. Gao, J. Guo, Z. Gao, Y. Huang, Z. Tu, and X. Liang, "High beam quality chirped pulse amplification laser based on plane-convex hybrid cavity Innoslab amplifier," Optics & Laser Technology 168, 109885 (2024). DOI: https://doi.org/https://doi.org/10.1016/j.optlastec.2023.109885

35. S.-B. Mansoor, A. S. Ali, J. H. David, M. J. Soileau, and W. V. S. Eric, "Nonlinear refraction and optical limiting in "thick" media," Optical Engineering 30, 1228-1235 (1991). DOI: https://doi.org/10.1117/12.55902

36. M. Sheik-Bahae, A. A. Said, T. H. Wei, D. J. Hagan, and E. W. V. Stryland, "Sensitive measurement of optical nonlinearities using a single beam," IEEE Journal of Quantum Electronics 26, 760-769 (1990). DOI: https://doi.org/10.1109/3.53394

37. A. Suda and T. Takeda, "Effects of Nonlinear Chirp on the Self-Phase Modulation of Ultrashort Optical Pulses," Applied Sciences 2(2012). DOI: https://doi.org/10.3390/app2020549

38. E. A. Khazanov, S. Y. Mironov, and G. Mourou, "Nonlinear compression of high-power laser pulses: compression after compressor approach," Physics-Uspekhi 62, 1096-1124 (2019). DOI: https://doi.org/10.3367/ufne.2019.05.038564